POLITECNICO DI MILANO
Laurea Magistrale (MSc) in Automation and Control Engineering
Dipartimento di Elettronica, Informazione e Bioingegneria (DEIB)

MODEL-BASED CONTROL OF AN ASYMMETRIC SHOCK TUBE EXPERIMENTAL FACILITY

Supervisor: Prof. Francesco Casella

Author of the thesis:
Luca Maggiolini Cacciamani, 713408

Accademic Year 2017-2018

Contents

List of Figures

Summary

The Flexible Asymmetric Shock Tube experimental facility, FAST, is used to conduct experiments on the expansion of non-ideal compressible fluid. It is composed of a vapour generator connected to a 9-m long pipe referred as charge tube, CT. Once the desired thermodynamic conditions are obtained in the charge tube a fast opening valve is opened and the fluid expands in a recipient at lower pressure creating a shock wave. Pressure transducers record the pressure differential moving along the charge tube. During the first experimental campaign, problems with the control design of the facility arose that made further experiments difficult. A model based control design approach is adopted to design a better control scheme for the FAST. The author of this thesis proposes a methodology for the creation of the set point curve of the vapour generator and a new control scheme for the reference tube, RT. The reference tube is a 0.5 m long tube, geometrically identical to the charge tube that is used as a reference for the control of the CT, having a temperature sensor immersed inside that in the CT it is not possible to have for experimental reasons. Previously the control of the RT used as process variable the difference between the temperature measurement of the fluid inside it and the saturation temperature of the fluid inside the vapour generator to control the desired superheating of the fluid inside the RT and CT. The control scheme that this thesis proposes make use of both the low-pass filtered measured temperature inside the RT and the high-pass filtered surface temperature of the RT so that the control is less sensible to the uncertainties of the fluid behaviour inside the RT. Simulations, using the FAST model, confirm the validity of the proposed control strategy.

Sommario

Il Flexible Asymmetric Shock Tube, FAST, è un apparato sperimentale usato per condurre esperimenti di espansione di fluidi comprimibili non ideali. È composto da un generatore di vapore connesso ad un tubo di 9 m di lunghezza a cui si fa riferimento come charge tube, CT. Una volta che le condizioni termodinamiche desiderate vengono raggiunte nel charge tube, una valvola ad apertura rapida, posta all'estremità del CT, si apre e il fluido si espande in un recipiente a pressione inferiore creando un'onda d'urto. Sensori di pressione posti lungo il charge tube misurano la variazione di pressione che risale il CT. Durante la prima campagna di esperimenti il controllo dell'apparato ha presentato numerosi problemi che hanno reso difficile l'esecuzione di ulteriori esperimenti. Lo scopo di questa tesi è proporre uno schema di controllo migliore per il FAST, progettando il controllo su un modello dell'apparato sperimentale. I principali cambiamenti proposti sono un metodo diverso per la creazione del set point del generatore di vapore e un nuovo schema di controllo per il reference tube, RT. Il reference tube è un tubo di 0.5 m utilizzato come riferimento per il controllo del CT avendo al suo interno un sensore di temperatura che nel CT non è possibile avere per ragioni sperimentali. Precedentemente il controllo del RT usava, come variabile di processo, la differenza fra la temperatura interna, misurata nel RT, e la temperatura di saturazione del fluido, misurata nel generatore di vapore, per controllare il grado di surriscaldamento desiderato nel RT e CT. Lo schema di controllo proposto per il RT utilizza invece una combinazione della temperatura interna al RT filtrata con un filtro passa basso e la temperatura della parete esterna del RT filtrata con un filtro passa alto in modo che lo schema di controllo sia meno sensibile alle incertezze legate al comportamento del fluido di lavoro all'interno del reference tube. Simulazioni, fatte con il modello del FAST, confermano la validità della strategia di controllo proposta.

Acknowledgements

My thanks go to Professor Casella. His help and patience was invaluable to the completion of this thesis.

Un ringraziamento particolare a mia madre e a mio padre per il loro sostegno in questi lunghi anni.

Chapter 1

Introduction

The Asymmetric Shock Tube Experimental Facility, referred in this paper as FAST, is an unconventional Ludwieg tube designed and installed at Delft University of Technology, in the Netherlands. The FAST consists of a vapour generator that evaporates an organic fluid, Siloxane D6. The fluid vapour flows to a tube, called charge tube, fitted with pressure sensors. Once the desired thermodynamic conditions are obtained in the charge tube a fast opening valve is opened at the end of it and pressurized fluid expands on a container at lower pressure, referred to as low pressure plenum. A picture of the apparatus is shown in figure 1.1.

The purpose of the FAST experimental apparatus is to test the actual occurrence of expansive shock waves. Zeldovich [1] theorized that shock waves can be both compressive and expansive depending on the sign of a quantity Γ In ideal gases, we have various examples of compressive shock waves: the flow of air around a supersonic aircraft and in supersonic turbines. On the contrary, the actual occurrence of rarefaction shock waves, RSWs, has never been verified, despite the theory on them being well established.

Γ is defined as

$$\Gamma \equiv 1 + \frac{\rho}{c}\left(\frac{\partial c}{\partial \rho}\right)_s \tag{1.1}$$

Where c is the speed of sound and s is the entropy.

In ideal gases rarefaction shock waves, RSWs, violate the second law of

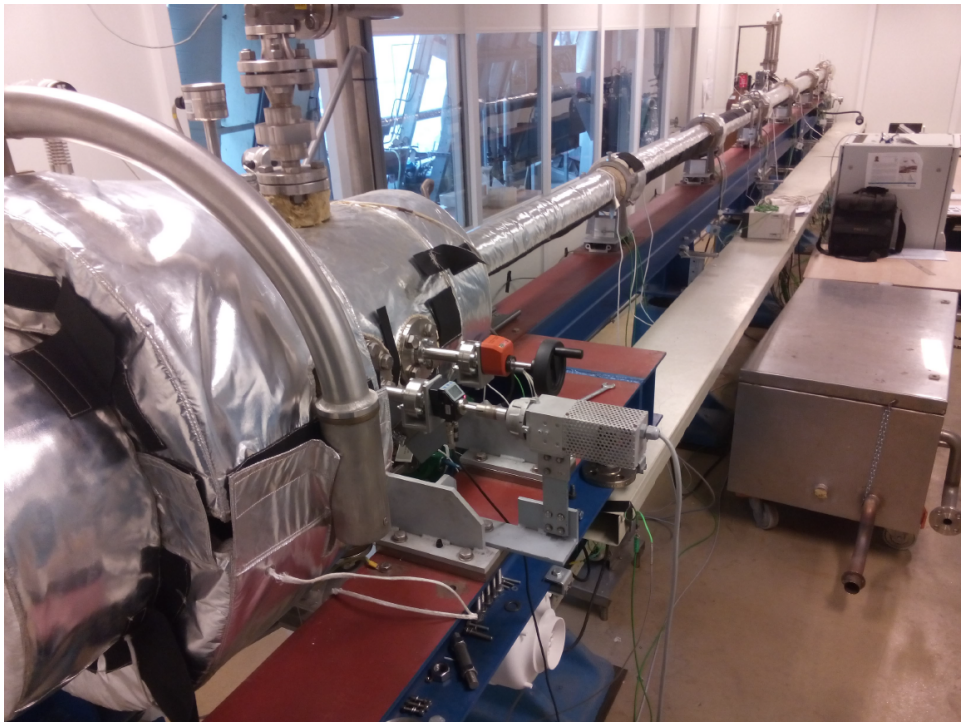

Figure 1.1: Picture of the FAST apparatus. In the foreground the low pressure plenum, in the background the charge tube

thermodynamics because they would cause a decrease in entropy through the shock wave. Therefore RSWs are not admissible in ideal gases. Thompson [2] theorizes that, for negative values of Γ, the constraint reverses and only RWSs are admissible.

Writing Γ in a more convenient way as a function of specific volume, speed of sound and pressure

$$\Gamma \equiv \frac{v^3}{2c^2}\left(\frac{\partial^2 P}{\partial v^2}\right)_s \tag{1.2}$$

It is apparent that in the thermodynamic P-v diagram of a fluid, see figure 1.2, that the curvature of the isentrope shows the sign of Γ, since c and v can only have positive value. The first region is in the two-phase regime, just below the critical point. The BZT region, named after scientists Bethe, Zelâdovich and Thompson, is a region of negative Γ predicted to occur in fluids formed by sufficiently complex molecules, like the one used in the FAST. It is located in the single-phase vapour region close to the dew line.

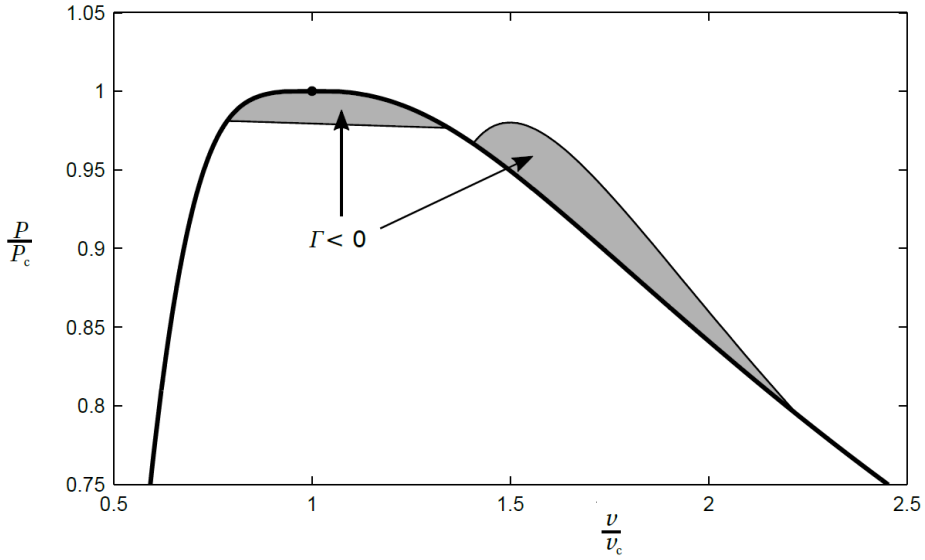

Figure 1.2: Pressure-volume diagram of a fluid, with the regions of negative Γ *highlighted.*

By bringing the fluid in the FAST to the predicted BZT region in the charge tube and then opening the valve connecting the charge tube to the low pressure plenum it is hoped to observe the formation of a backward RSW in the charge tube. In figure 1.3 is shown a schematic overview of a rarefaction wave experiment. The first chart shows the qualitative profile of pressure inside the charge tube after the opening of the valve separating it from the low pressure plenum. In black and in red are indicated the two kind of behaviour possible: a standard rarefaction fan and a rarefaction shock wave. Pressure is measured by pressure transducers along the charge tube.

The initial set of experiments using the FAST and a thorough description of the conditions necessary for the formation of a RSW in the FAST are detailed in *Experimental observation of non-ideal compressible fluid dynamics* by Tiemo Mathijssen [3]. The initial set of experiments was not followed by more in depth research because the reliability with which the FAST was able to bring the fluid to the prescribed conditions was completely insufficient.

The objective of this thesis is to provide a better control design for the FAST without proceeding by trials and errors directly on the facility. Instead, a model-based approach is used. If the assumptions and simplifications made on the model are correct, once a simple validation of some parameters is done, the control design could be directly adopted and provide the necessary

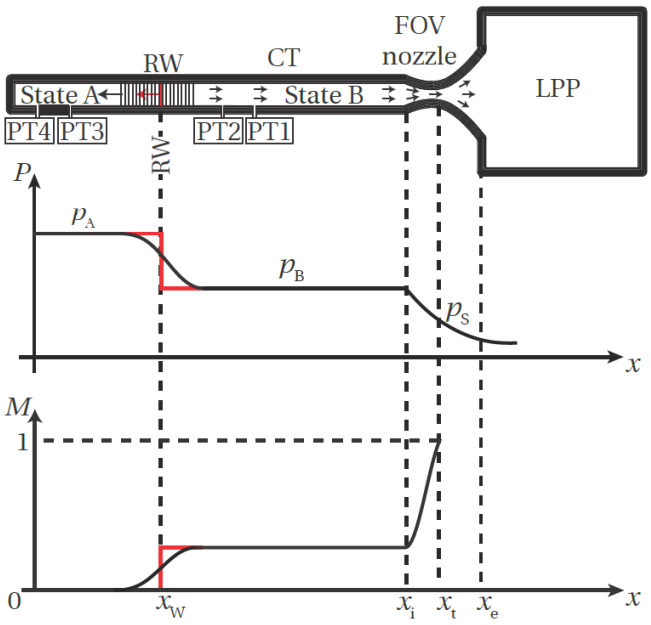

Figure 1.3: Schematic overview of a rarefaction wave experiment

foundation to proceed with a new experimental campaign to investigate further rarefaction shock waves.

1.1 Outline of the thesis

Chapter 2 describes the FAST experimental apparatus and the control problem with its objectives and constraints. Chapter 3 describes the Modelica model used to simulate the FAST. Chapter 4 describes the control design and presents simulation results using the proposed control schemes. Chapter 5 presents the conclusions and an outlook into future developments of the FAST facility.

Chapter 2

The FAST facility

This chapter describes the FAST experimental apparatus, especially those components that are meaningful for the control problem. A subsequent section presents the control problem: the objectives and the constraints of designing a control scheme for the FAST.

2.1 The experimental apparatus

In this chapter it is described the process that the Siloxane D6 fluid undergoes in the FAST experimental facility. Preliminary operations to purify the fluid and prepare the facility are omitted since they are not relevant to the scope of this thesis. The layout of the FAST experimental apparatus is shown in Figure 2.1.

Firstly, after the preliminary operations, the working fluid is let flow into the vapour generator, also referred to in this paper as heated fluid tank or HFT. The vapour generator is a 5.9 stainless steel vessel. Its purpose is to heat and evaporate the fluid under isochoric conditions. Initially the total volume is the one of the vapour generator then, once the MV-4 valve is opened, the vapour will flow in the reference tube and charge tube.

The heating of the fluid in the vapour generator is obtained using a 1.5-kW ceramic band heater covering the elongated part of the tank, where the fluid is always in liquid phase thus guaranteeing a high heat transfer coefficient. This heater is referred in this paper as lower band heater or LBH. Also the

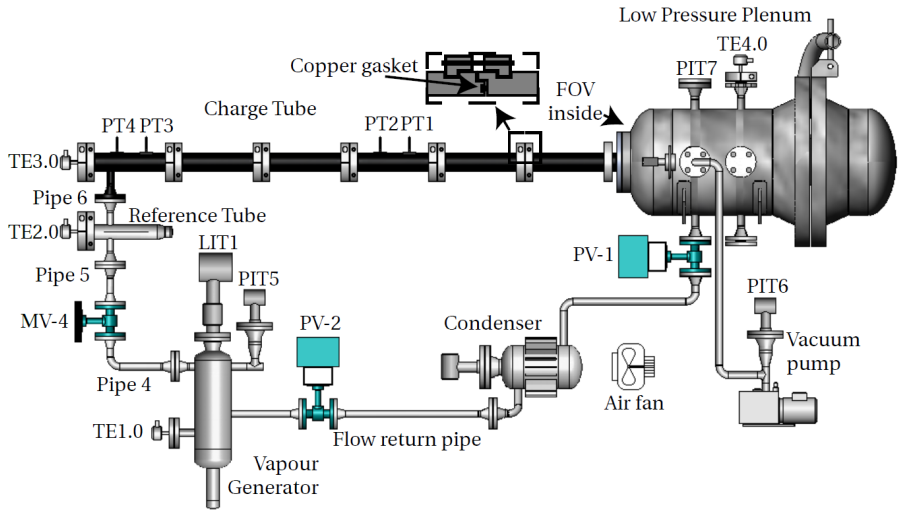

Figure 2.1: Overview scheme of the FAST

risk of thermal decomposition of the fluid is avoided by providing all the heat to the fluid in that section of the HFT. Between the band heater and the metal wall of the vapour generator there is a 2-mm graphite layer that ensues uniform surface temperature distribution.

The vapour generator has two other heaters, one in the central section of the tank and another in the top. These two heaters are used to control the temperature of the walls so that they are slightly colder than the fluid inside to favour condensation; the fluid then flows back to the bulk. This process of convective heat transfer should ensure that there is thermodynamic equilibrium inside the tank. The central heater is also a 2.8-kW ceramic band heater coupled with a 2-mm graphite layer and is referred as upper band heater or UBH. At the top of the vessel, because of space constraints, is instead coiled a 6-m 1-kW Joule dissipating heating wire once again in combination with a 2-mm graphite layer. This heating device is referred as top heater wire of THW. Similar heating wires are also placed around all flanges leaving the HFT to ensure uniform temperature distribution. The vapour generator is isolated with a 50-mm thick layer of rockwool insulation. The HFT is fitted with an immersion temperature sensor and a pressure sensor. Thermocouples also measure the wall surface temperature in all three sections of the HFT.

Once a threshold pressure is obtained in the HFT, a manually operated

19.05-mm globe valve is opened and fluid vapour flows through pipe 4 to the reference tube and the charge tube, see figure 2.1. The valve is referred in figure 2.1 as MV-4. MV4 is also the name that indicates the ON/OFF command that operates the opening of the valve in the model. The valve is referred in this paper also as HFT_Valve.

The reference tube, also referred to as RT, is a 0.5-m long tube with an internal diameter of 40-mm and 15-mm thick walls. The thickness of the walls allows an even distribution of the thermal power provided by a 335 W heating jacket placed around the tube. A 20-mm rockwool insulation layer is present between the RT and the heater and between the heater and external air. The reference tube is fitted with an immersion temperature sensor and a 1-mm thick thermocouple between the insulation layer and the metal wall.

The charge tube, also referred to as CT, has the same geometry of the RT, but is composed of six sections each 1.52-m long. Each section is fitted with a 950 W heating jacket and surface temperature thermocouple. There is no immersion temperature sensor in order not to disturb the flow of the fluid during the expansion wave propagation inside the CT.

The CT sections have a male-to-female connection, referred as charge tube joint or CTJ, where they overlap by 20-mm. The male side has a groove accomodating a copper seal. A coupling holds together the two segments and a 170 W Joule heating electric wire is placed around it so that there are no cold spot along the whole length of the CT. The total dimension of the CTJ is an equivalent pipe thickness of 55-mm. Rockwool insulation and a thermocouple to measure the outer surface wall temperature is also present.

The end of the CT is closed off by the fast opening valve, FOV, that connects it to the low pressure plenum, LPP. During the experiment, once the desired thermodynamic condition are obtained in the CT, the FOV is opened and the fluid expands in the LPP. Pressure sensors along the CT measure the pressure differential. The fluid is then condensed and collected so that it can flow in the HFT once again. The FOV is of paramount importance for the experimental apparatus, but not inherent to the scope of this thesis. For more details on the FOV and all other components of the FAST not described here see Mathijssen et al. *The flexible asymmetric shock tube (FAST), a Ludwieg tube facility for wave propagation measurements in high-temperature vapours of organic fluids* [5]

2.2 The control problem

The objective of the control of the FAST is to bring the fluid inside the charge tube in the BZT region. The BZT region is not well defined, at the moment, for the Siloxane D6 fluid, so in future experimental campaigns it will have to be investigated further. The region should lie close to the saturation curve with some degree of superheating and close to critical pressure. From a control perspective this means that the objective in terms of set points is not precisely defined.

Reviewing the experimental data on the first experimental campaign [3], see figure 2.2, the control objective is twofold:

no	P_{HFT} [bar]	T_{HFT} [bar]	T_{CT} [°C]	ΔT_{sup} [°C]	Γ [-]	c [m/s]
1	8.40	365.6	367.6	2.00	0.132	51.2
2	8.47	365.4	367.5	1.95	0.086	49.7
3	8.56	367.3	367.8	0.51	0.057	48.6
4	8.79	368.0	368.8	0.84	-0.019	45.5
5	8.80	368.3	369.0	0.66	-0.012	45.7

Figure 2.2: Thermodynamic conditions of the FAST before the opening of the FOV during the experimental campaign

1. Reaching a pressure P_{HFT} in the neighbourhood of 8.5 bar with a corresponding saturation temperature T_{HFT} in the neighbourhood of 367°C
2. Reaching a ΔT_{sup} in the neighbourhood of 1°C. ΔT_{sup} is the superheating degree that the fluid undergoes inside the charge tube.

The first objective is reached by closing a control loop, either around the pressure, or the temperature of the vapour generator.

The second objective is reached by controlling the temperature of the fluid inside the reference tube. The reference tube is geometrically identical to the charge tube, except in length. It is used for this reason as a reference for the control of the charge tube having an immersion temperature in its

central cavity that the charge tube lacks because it would disturb the flow of the shock waves.

Furthermore there are a number of constraints to how this objectives are to be reached:

1. The fluid must not be in contact in its vapour phase with wall temperatures of 375°C or more since fluid degradation can occur. Therefore special precaution must be used while superheating the fluid in the reference and charge tube that pipe walls never reach such temperatures. If the fluid is to reach those temperatures the FAST would have to be purged of all the fluid and cleaned thoroughly at great expense of money and time. This temperature threshold is taken only as a reference since the actual behaviour of the fluid is not well known in this respect.

2. The fluid must not be permitted to condensate while being outside of the vapour generator, in the reference tube and charge tube. Once condensation starts to occur a local cold spot is formed that would become the catalyst for further condensation. The accumulated condensate would have to be purged in order to proceed with the experimental campaign.

Chapter 3

The FAST model

The model of the plant is written in Modelica language, an object-oriented, declarative modeling language for component-oriented modeling of complex systems. The model was originally written by Professor Francesco Casella to test different control design of the FAST experimental apparatus. The model makes use of the ThermoPower library, an open Modelica library for the dynamic modeling of thermal power plants [6, 7, 8]. It provides a library of component models that are used in the FAST model. The model also makes use of the FluidProp tool and library [4]. It is used to compute the thermodynamic properties of the Siloxane D6 fluid used as the medium in the experimental facility.

The overall scheme of the model is displayed in figure 3.1. The vapour generator, HFT, on the bottom left, is connected to the HFT_Valve. From there to the reference tube, RT, and the charge tube, CT. In the model overview, another pipe component that represents the charge tube joints, CTJ, is also visible. The low pressure plenum, the condenser and all other components that do not have an impact on the control problem are of course not present in this model.

The overall modelling assumptions underlying the model are the following:

1. The model of the heat distribution in the pipes is in principle 2D. The first dimension is radial, the second one longitudinal with respect to the length of the RT and CT pipes. In order to make the model

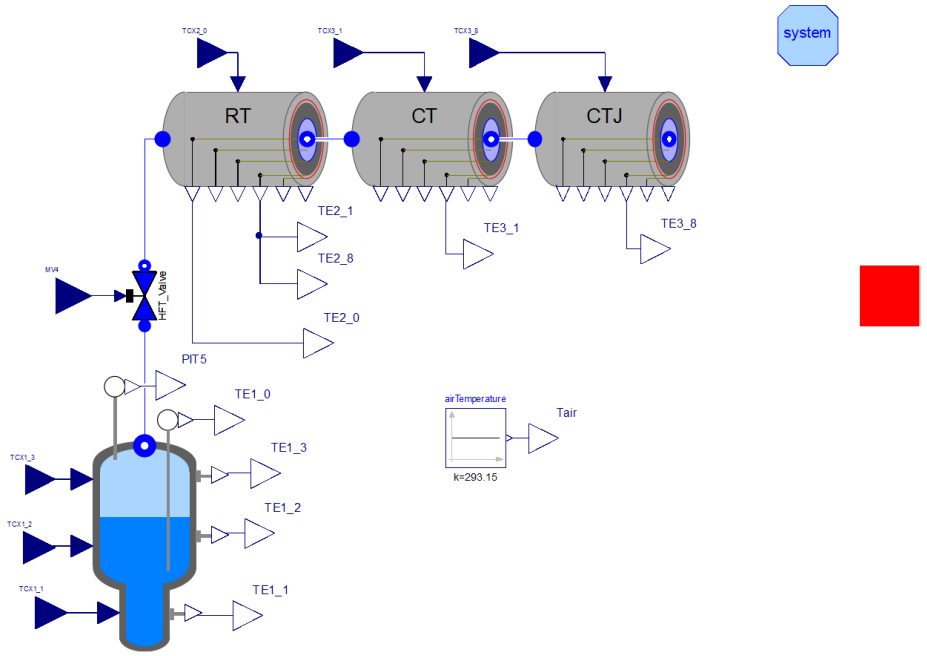

Figure 3.1: Overview scheme of the plant model

computationally less taxing, the longitudinal dimension is discarded assuming that there is no significant heat gradient along the CT pipe. This modelling hypothesis is guaranteed valid by the temperature control used in the CT that maintains the walls of the CT at a slightly higher temperature than the incoming fluid. The high heat capacity of the walls together with the low heat capacity of the fluid already present in any given section of the tubes makes the slight difference in temperature of the incoming fluid negligible, hence the model becomes 0D along the longitudinal axis. Because of this, the thermal flow between pipe and gas is negligible compared to the thermal flow of the pipe heaters. The control of the CT is discussed in depth in chapter 4.

2. Since the model is 0D along the longitudinal axis the order in which joints CTJ and pipe sections CT are positioned is not important. See figure 3.1. The CT element represents 6 identical pipe sections in succession, while the CTJ element represents 7 identical joints in succession. There is no heat exchange between each section on the longitudinal axis because the thermal coupling in the longitudinal direction is extremely slow, compared to the time scale of interest for control.

In the FAST facility each pipe section and joint would have is own proper position and controller, but since they are assumed identical in the model, the order does not matter and only one controller per CT section and CTJ section is implemented.

3. Heat losses and pressure drops through the connecting pipes, from the HFT to the RT and from the RT to the CT, are negligible, hence they are not modelled.

4. The pipe supports are considered fully isolated. Introducing heat losses through the support would introduce a discontinuity on the 1D radial model of the thermal distribution in the pipes. It is neglected, since it is assumed small, for simplicity.

In the following chapters the two major elements of the model will be briefly described: the vapour generator and a generic pipe section, since RT CT and CTJ share the same model with different parameters.

Below, the outputs and inputs representing the signals of sensors and actuators relative to the vapour generator, HFT_Valve, reference tube, charge tube and joints are listed as a reference guide.

- TE1_0 is the PT100 temperature sensor output located inside the HFT fluid in liquid phase.
- PIT5 is the PIT5 pressure sensor output located inside the HFT fluid in vapour phase.
- TE1_1, TE1_2 and TE1_3 are the output of the thermocouples positioned in the outer surface of the HFT.
- TCX1_1, TCX1_2 and TCX1_3 are the input signals of the heaters of the HFT walls.
- TE2_0 is the PT100 temperature sensor output located inside the reference tube, RT.
- TE2_1 and TE2_8 represent the same signal, i.e. the output of the thermocouple positioned in the outer surface of the reference tube, RT.
- TCX2_0 is the input signal of the heater of the reference tube walls.

- TE3_1 represents the output of the thermocouple positioned in the outer surface of the first section, and only section modelled, of the charge tube, CT.
- TCX3_1 is the input signals of the heater of the section 1 of the CT.
- TE3_8 represents the output of the thermocouple positioned in the outer surface of the first charge tube joint, the only joint modelled, CTJ.
- TCX3_8 is the input signals of the heater of the charge tube joint.
- MV4 is the ON/OFF command of the HFT_Valve.

3.1 The heated fluid tank model

An overall view of the heated fluid tank, HFT, is displayed In figure 3.2.

The HFT is modelled as a 0D two-phase volume at thermodynamic equilibrium. The thermodynamic properties are obtained through lumped parameters mass balance equation and energy balance equation. The model assumes isothermal condition of the fluid and perfect phase separation, i.e. the volume of vapor bubbles in the liquid phase and condensed liquid is negligible.

The only variation of mass is due to the fluid vapour leaving the vapour generator from the outlet flange connector.

The variation of energy are due to the heat contribution of the lower band heater LBH, upper band heater UBH, top heater wire THW and energy loss due to the enthalpy of the fluid leaving the HFT.

The ceramic band heater LBH supplies most of the power, being directly in contact with the elongated section of the HFT that always contains fluid at the liquid phase. It is modelled as two 0D masses with a constant heat capacity: the first one representing the lower section of the HFT metal walls with heat capacity Cw_LBH, the second one representing the mass of the ceramic band heater with heat capacity C_LBH. Connected to the second mass we have the heater that inject heat in the mass proportional to the actuator signal TCX1_1 and the wall temperature sensor. Between the two masses is present an air gap modelled as a lumped parameter convective

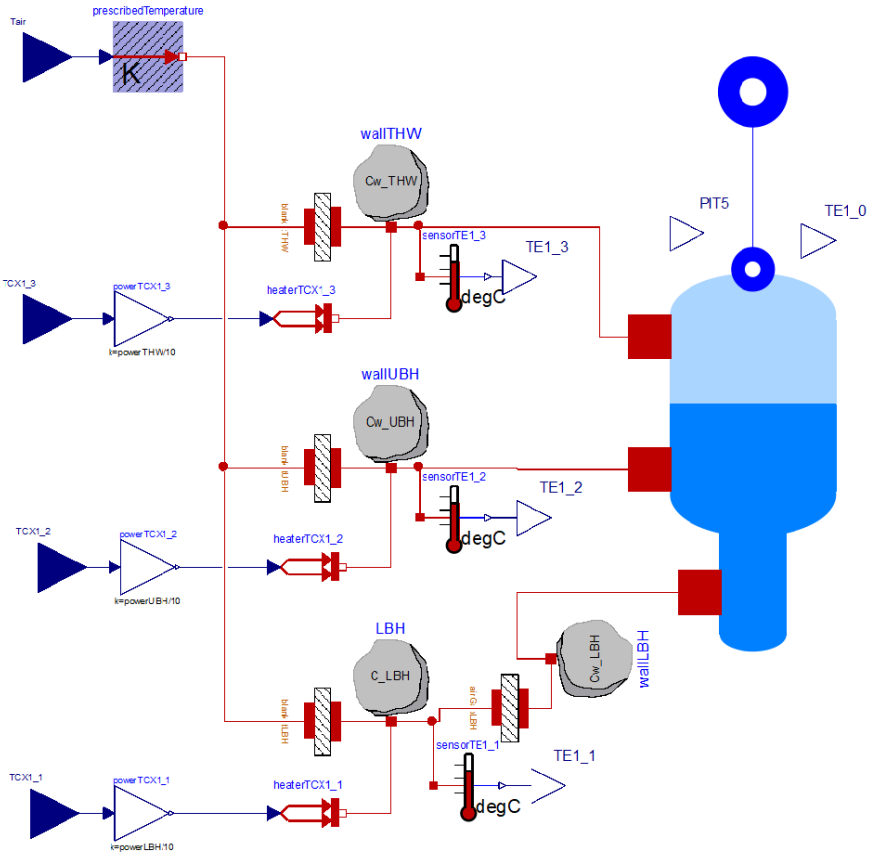

Figure 3.2: Overview scheme of the heated fluid tank model

heat transfer with a constant thermal conductance. Similarly, heat dissipation through the insulating rockwool blanket is modelled as convective heat transfer.

The upper band heater and top heating wire are modelled the same way except that the heat is supplied directly to the corresponding wall section of the HFT.

The walls of the HFT are not modelled using Fourier equations since a precise control of their temperature is not necessary and also the thickness is considerably smaller compared to the one of the reference tube and charge tube, therefore a lumped parameters approximation is deemed a good approximation.

3.2 The insulated heated tube model

The model of the insulated heated tube class is displayed In figure 3.3. The parameters of the class are then changed in order to create the RT, CT and CTJ model, varying the geometrical properties, the presence or absence of the internal PT100 temperature sensor and the nominal power of the heaters.

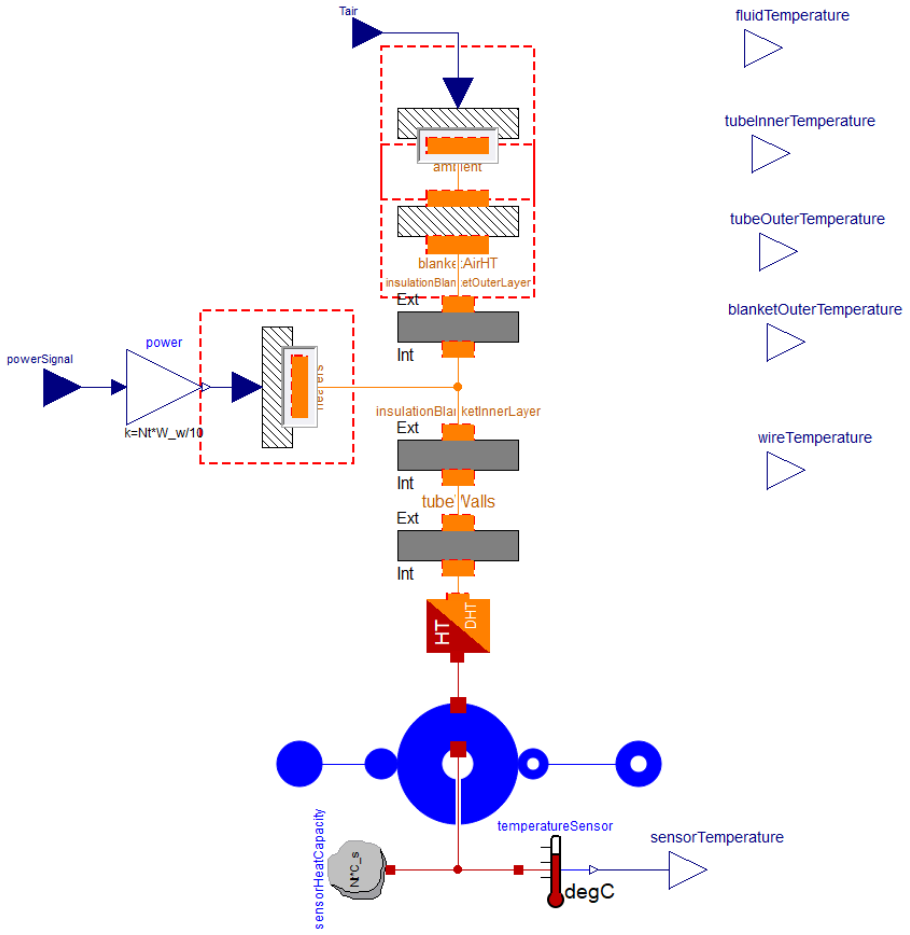

Figure 3.3: Overview scheme of the insulated heated tube model

The fluid volume is modelled as a hollow cylinder of well-mixed fluid. The cylindrical cavity at the center is used to allow for the presence of the PT100 temperature sensor, modelled as a 0D mass lumped thermal element storing heat and a temperature sensor. The model of the CT and CTJ, that do

not have a temperature sensor, have the cylindrical cavity created with a diameter of 10^{-6} [m] so that it is negligible . The thermodynamic properties are obtained through lumped parameters mass balance equation and energy balance equation.

The only variation of mass is due to the fluid vapour entering or leaving the pipe section.

The variation of energy are due to the heat power of the heating element of the section of the tube and energy loss due to the enthalpy of the fluid entering or leaving the the pipe section.

Connected to the fluid volume is the discretized representation of the pipe wall in the radial direction. The temperature distribution is obtained using the finite differences Fourier equations in each of the layers: the metal wall of the pipe, the inner layer of rockwool insulation and the outer layer of rockwool insulation. The heating element of the pipe is connected between the two insulating layers, while the heat loss through air is connected to the external layer of insulation.

Each metal and insulating layer is discretized in a suitable number of layers to provide an accurate thermal model of the pipe walls since the wall temperature dynamics is of paramount importance for the control.

Chapter 4

Control design

The overall control architecture of the FAST is displayed in figure 4.1. It is designed and implemented as a distributed control system for simplicity reasons. The red connections represent bus connection that exchange data from sensors and actuators between the controllers and the plant.

The state of the art of the FAST control architecture, proposed originally by N. R. Nannan in *Advancements in nonclassical gas dynamics* [9], is discussed in this chapter together with the improvements that are proposed in this thesis.

- TC1_1 is the controller of the vapour generator lower band heater whose purpose is to regulate the heating of the fluid inside the HFT.
- TC1_2 and TC1_3 are, respectively, the controller of the upper band heater and top heater wire; their purpose is to regulate the temperature of the HFT walls in contact with the fluid vapour.
- TC2_0 is the controller of the reference tube RT thermal jacket whose purpose is to finely control the degree of desired overheating of the fluid in the RT and to ensure that the pipe walls are always at a higher temperature than the saturation temperature of the fluid. Since the temperature control of subsequent tube sections of the charge tube and charge tube joints all match the external surface temperature of the RT, TC2_0 is the main temperature control of the experimental apparatus.

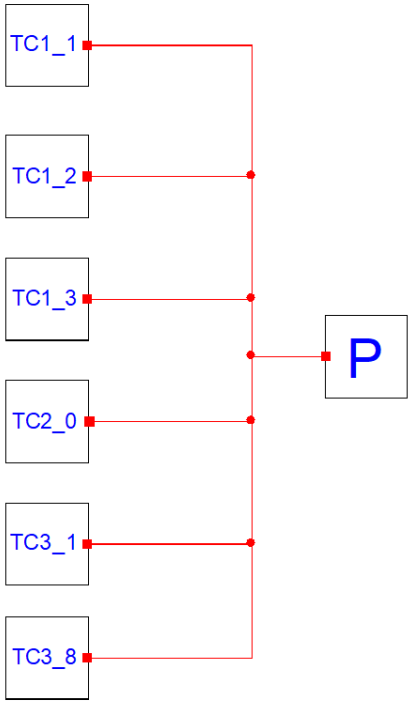

Figure 4.1: Overview scheme of the plant control

- TC3_1 is the controller of the thermal jacket of the first section of the charge tube CT. Its purpose is to keep the CT pipe walls at the same surface temperature of the RT pipe walls. Controllers TC3_2 through TC3_6 are not represented since they would be identical and would act identically because of the modelling assumption of longitudinal isothermic distribution. In the simulation, each of the six CT section is controlled by the same TC3_1 controller.

- TC3_8 is the controller of the first charge tube joint CTJ. Its purpose is analogue to the one of CT3_1, i.e. to keep the CTJ pipe walls at the same surface temperature of the RT pipe walls. CT3_8 is also used as the controller of all seven charge tube joints substituting CT3_9 through CT3_14.

In the following sections each control design is described in depth.

4.1 HFT fluid saturation temperature control

The control scheme of the lower band heater LBH of the vapour generator HFT is displayed in figure 4.2. The ceramic plate heater LBH is chosen as the main heater of the HFT since it is positioned around the elongated bulk of the tank, the part that is always in contact with the fluid in liquid phase. The advantages of this choice are the high thermal exchange coefficient between liquid and metal wall, due to the boiling regime, and the prevention of fluid degradation caused by excessive wall temperature, the fluid being only in liquid phase.

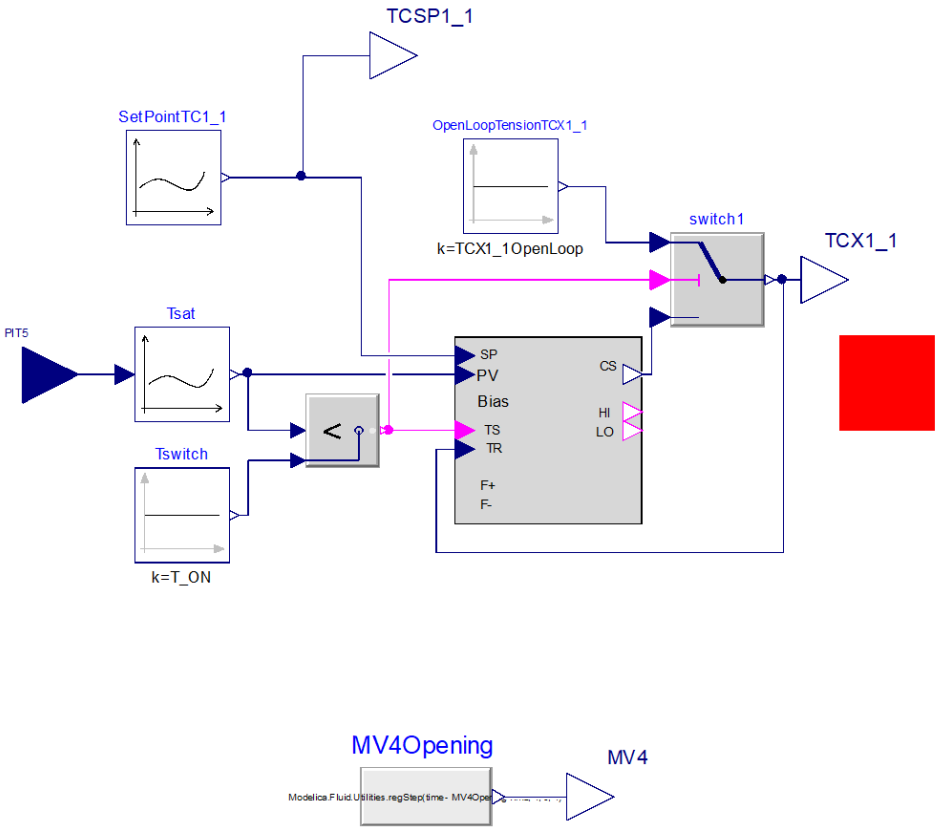

Figure 4.2: Overview scheme of the HFT LBH control

The control operates in two modes: feed-forward mode and PID control mode. The need for having two modes arises from the unreliability of the pressure sensor at low pressures, under 1 bar. Based on simulations of the HFT model, a saturation temperature value of the fluid, Tswitch, is determ-

ined such that the pressure inside the HFT will be over 1.2 bar. Switching from feed-forward mode to PID mode occurs when the saturation temperature is greater than Tswitch. In feed-forward mode, the initial condition of Switch1, the control operates in open loop and outputs a fixed value for the lower band heater LBH voltage. This value is obtained, once again, from simulations so that the process variable is sufficiently close to the value of the set point when the transition occurs.

In PID mode a suitable control scheme operates the controller. The process variable of the PID control is the saturation temperature calculated from the pressure sensor PIT5.

The operating pressure range of the HFT is wide, spanning from ambient pressure to close to critical conditions. If we were to control the HFT using the inside pressure as process variable, the output of the controller would change drastically because of the variation of the pressure derivative with respect to temperature at constant specific volume $(\frac{\partial P}{\partial T})_v$. Accordingly, the PID parameters would also have to be changed depending on the operating pressure range. This complicated process is avoided altogether by converting the pressure measurement to the corresponding saturation temperature using the FluidProp software. The pressure saturation temperature correspondence is then implemented as a look-up table once the control architecture is implemented in LabView. The control loop is now closed around the saturation temperature, since the specific heat capacity variation is less significant. The fluid mass variation due to evaporation is not negligible, but for the purpose of the HFT control, a fixed parameters PID is adequate, as verified in simulation. At the same time the fast response of the pressure sensor is still used for the control of the HFT.

4.1.1 HFT Set Point Curve

Of particular importance is the definition of the set point curve of the HFT controller since the set point of the reference tube RT is built adding a given superheating value to the HFT set point curve. Previously the set point curve was defined as a series of two steps: the first one to reach the pressure necessary to open the HFT_Valve, the second one to reach the desired maximum value of saturation temperature inside the HFT. This set point caused the saturation of the actuators at the start of the simulation, it took unnecessary long time around the HFT_Valve opening and the dis-

continuity between the final ramp and desired steady state value caused undesired overshoots of the fluid temperature.

The adoption of a curve that is better suited to the FAST control requirements is proposed in this thesis.

The proposed set point curve is generated from a set of points using a spline function that interpolates them. The resulting curve utilized as a set point is displayed in figure 4.3. The points generating the curve are obtained from a Matlab script, see appendix A, starting from a set of variables, both user-defined and fixed. These variables are used to create a ramp of varying first order derivative.

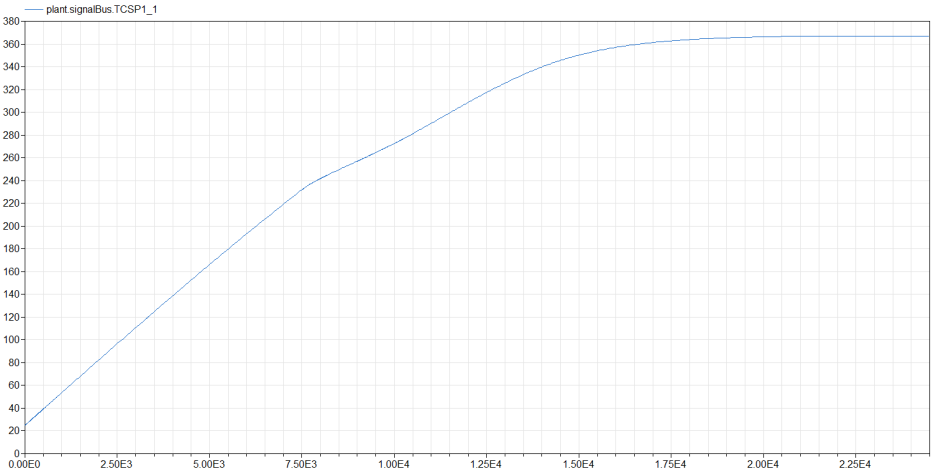

Figure 4.3: HFT set point curve

The first main user-defined variable is the time when the HFT_Valve is going to be opened, tmv4. By that time a specific temperature Tmv4 needs to be already reached so that the pressure inside the HFT is at the desired level. The value of Tmv4 is obtained from the model simulation. In the neighbourhood of tmv4 the ramp derivative is set at a fixed value so that the control signal of the thermal jackets does not exceed a given value. Given all these parameters the rate of the first branch of the curve is calculated.

The second main parameter is the total time of the process tmax when the saturation temperature of the fluid inside the HFT has to be the desired steady state value ThftMax.

The way the derivative of the ramp approaches zero is mapped from the derivative of an hyperbolic tangent so that the curve, the first derivative of

the curve, and the second derivative are without strong discontinuities. The third main parameter is how much time the ramp derivative takes to go to zero at the end of the transient.

From these three parameters the rate of the set point ramp in the first and third ramp sections are calculated and a suitable set of points is produced.

By manipulating the three variables and running simulations a good approximation of the best curve is obtained. What parameters are evaluated to find the optimal curve is discussed in section 4.6.

4.1.2 PID Tuning

A simplified model of the HFT, defined as follows, is used to tune the PID parameters using the Control System Toolbox of Mathworks.

$$\begin{cases} c_w \frac{dT_w}{dt} = Q - (T_w - T_{amb})G_{loss} + G_{wf}(T_f - T_w) \\ c_f \frac{dT_f}{dt} = G_{wf}(T_w - T_f) \end{cases} \tag{4.1}$$

c_w and c_f are the wall and fluid in liquid phase thermal capacitance. T_w and T_f are the wall and fluid temperature. G_{loss} is the thermal conductance representing convective heat transfer between metal wall and external air. Q represents the ceramic band heater heat flow. Finally G_{wf} is the thermal conductance representing convective heat transfer between metal wall and fluid.

Bumpless control transfer between feed-forward mode and PID mode is achieved using the output signal as tracking reference to the PID control.

4.2 HFT walls temperature control

The control scheme of the upper band heater is displayed in figure 4.4. The purpose of this control is to keep the upper wall section of the HFT at a slightly lower temperature compared to the measured temperature of the fluid. This is done to accumulate condensed fluid on the side walls that flows back in the bulk facilitating thermodynamic equilibrium inside the HFT. This avoid stratification phenomena.

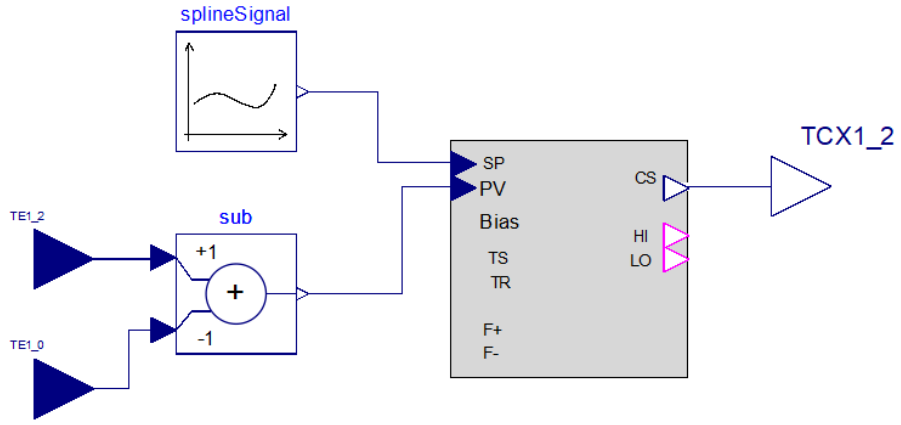

Figure 4.4: Overview scheme of the HFT TBH control

The process variable PV is the difference between the measured wall temperature in the upper section of the HFT and the measured bulk temperature of the fluid. The set point is the desired temperature difference.

A simplified model of the HFT wall, defined as follows, is used to tune the PID parameters using the Matlab Control System Toolbox.

$$c_w \frac{dT_w}{dt} = Q \tag{4.2}$$

c_w is the wall thermal capacitance. T_w is the wall temperature. Q represents the ceramic band heater heat flow.

The top wire heater controller works similarly so it will not be discussed any further.

4.3 RT temperature control

As already described in section 2.2, the geometry of the charge tube is identical to the one of the reference tube. Since it is possible to have an internal temperature sensor only in the RT, the controllers of the heating jackets of the CT will maintain the same external wall temperature of the

RT, therefore the control of the reference tube is the most important controller of all the experimental apparatus.

In the previous version of the FAST control architecture, the control design of the reference tube was very different: the process variable was the difference between the temperature measured inside the RT and the temperature measured inside the HFT, while the set point was a fixed delta of temperature, see figure 4.5. This version of the control did not manage well the superheating of the fluid in the neighbourhood of Tmax. Since the fluid temperature inside the RT lags behind the RT wall temperature, the control signal would gradually increase the external wall temperature at levels in which the Siloxane degrades. Further problems, not directly visible in simulation, are the unreliability of the temperature measurement TC2_0 while the RT is almost empty of any fluid before the HFT_Valve opening and the use of TC1_0 that would add the sensor uncertainties of the HFT to the RT without significant benefits during the temperature ascent to Tmax.

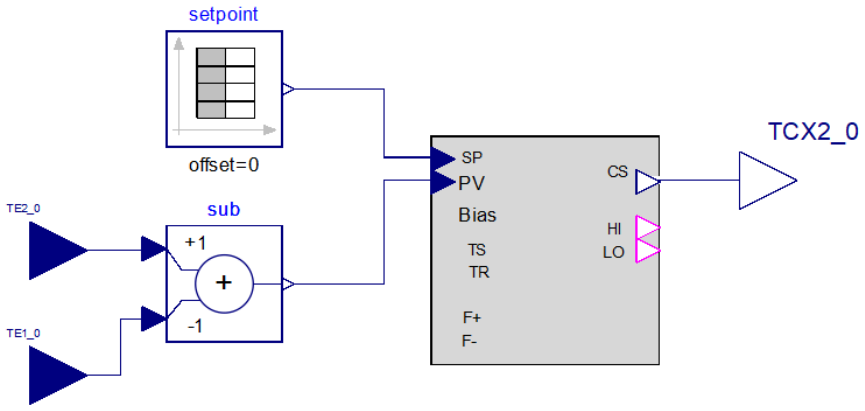

Figure 4.5: Previous version of the RT control design

In this thesis, a different control strategy is proposed. The purpose of this control is threefold:

1. Always guarantee that the internal walls of the RT, CT and CTJs are at a higher temperature with respect to the saturation temperature of the fluid at that given pressure to avoid superficial condensation on

the walls.

2. Provide the amount of superheating requested by the current experiment set at the end of the transient, Tsurr.

3. Always guarantee that the walls of the tubes are at a lower temperature than 375°C. The exact temperature at which the Siloxane D6 degrades is not precisely known, but this value is adopted as a safe margin nonetheless.

The requirement that the fluid inside the RT and the CT be always at a fixed temperature differential with respect to the HFT is dropped since during the transient it is of no importance the exact value. Also the HFT set point temperature is used for most of the transient, instead of always using the measured temperature of the HFT. Assuming the control of the HFT temperature is stable and robust, introducing the sensor delays and uncertainties of the HFT temperature sensor is unnecessary.

4.3.1 RT electric equivalent

In order to better understand how to design the RT control, an electric equivalent of the thermal model of the reference tube is built, see figure 4.6.

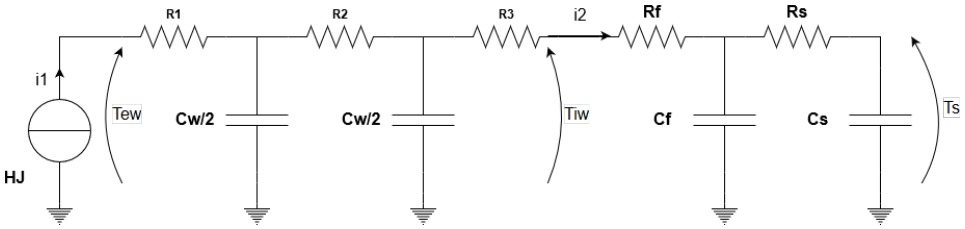

Figure 4.6: Equivalent circuit of the RT model

Voltages Tew and Tiw represents the temperature of external and internal wall of the pipe. Voltage Ts represents the measured temperature of the fluid inside the RT. The current i1 represents the thermal power of the heat jacket around the RT. R1, R2 and R3 represents the thermal resistance of the metal pipe, while Rf represents the thermal resistance of the natural convection between the fluid and the internal metal wall. Finally Rs represents the thermal resistance of the convective heat exchange between the fluid and the temperature sensor inside the RT. The capacitors represent the thermal capacity of each element of the model: the pipe wall, the fluid and the

sensor. The metal pipe is divided in two sections to better represent the behaviour of the pipe wall. Heat loss through air is neglected since it would only slightly decrease the output of the ideal current generator.

From the model it is possible to observe we have a series connection of four RC circuits. Of the first two we know very well all parameters: the prescribed heat power is known, while the Fourier equation for the distribution of heat in a solids allows us to well approximate all other parameters. On the contrary, the parameters of the two other RC circuits are very uncertain: the thermal resistance due to convection is not well known and varies depending of the fluid density, that varies during the transient. Also the heat capacity of the fluid varies greatly during the transient.

Nevertheless, the approximate values of Rf and Rs are very big compared to the one of the metal, while the thermal capacity of the fluid and sensor are small compared to the one of the metal wall. Consequently the current i2 is negligible during the transient, while the first two capacitors are charging; it is possible to approximate the second part of the circuit as if it did not load the first part at all.

Therefore it makes sense to close the loop around the first well known part of the circuit, while the second part could remain in open loop. At steady state the temperature would become the same. This control rule that favours the walls of the RT is in accordance to the design principles defined precedently.

Based on these observation of the electrical equivalent of the thermal model of the RT, the control design of the RT is defined as follows.

Given the thermal model so defined, neglecting for simplicity also the sensor and R1 and R3:

$$\begin{cases} \frac{c_w}{2}\frac{dT_{w1}}{dt} = Q + (T_{w2} - T_{w1})G_w \\ \frac{c_w}{2}\frac{dT_{w2}}{dt} = (T_{w1} - T_{w1})G_{w2} + (T_f - T_{w2})G_{wf} \\ c_f\frac{dT_f}{dt} = (T_{w2} - T_f)G_{wf} \end{cases} \tag{4.3}$$

Gw1 is the transfer function between the external wall temperature and heat impressed, while Gf is the transfer function between the fluid temperature and impressed heat.

$$
\begin{aligned}
G^*(s) &= \frac{1}{s\frac{c_w}{2}} \\
G_{w1}(s) &= G^*(s)G1(s) = \frac{1}{s\frac{c_w}{2}} \frac{(1+\tau_1 s)(1+\tau_2 s)}{(1+T_1 s)(1+T_2 s)} \\
G_f(s) &= G^*(s)G2(s) = \frac{1}{s\frac{c_w}{2}} \frac{1}{k} \frac{1}{(1+T_1 s)(1+T_2 s)}
\end{aligned} \tag{4.4}
$$

It is important to note that T_2 represents the time constant of the slowest pole. It is dependent upon c_f and G_{wf}. As already discussed these two parameters are uncertain in the model and variable. In the case of G_{w1}, T_2 is cancelled by τ_2 that has almost the same value. This confirms the assumption made in the electrical equivalent model that the second half of the circuit does not impact on the first half. On the contrary, T_2 remains in G_f.

In figure 4.7 is shown the block diagram of the RT control.

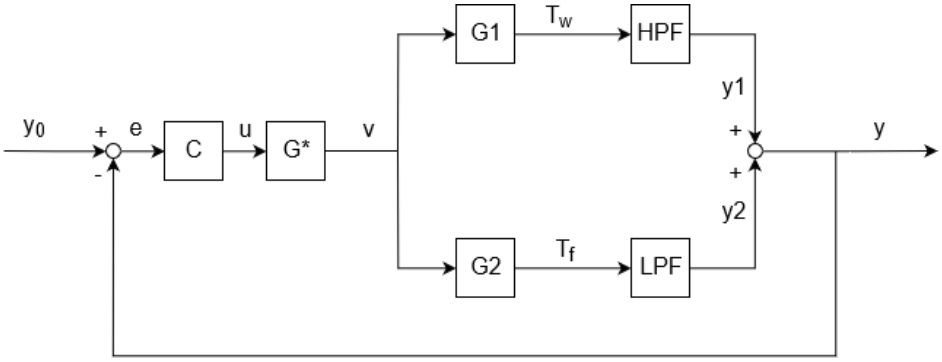

Figure 4.7: Block diagram of the proposed RT control design

Instead of using only the measurement of the fluid temperature, a combination of the low pass filtered fluid temperature measurement Tf and the high pass filtered external wall temperature measurement Tw1 is used to obtain the error e. The cutoff time of the filters Tf is chosen so that the prevalent dynamic is the one of the external wall. The internal fluid temperature is not left in open loop so that a more precise steady state control of the internal fluid is possible, in accordance of the design principles.

More precisely Tf is chosen following two conditions:

1. $\frac{1}{T_f} \ll \omega_c$
2. $\frac{1}{T_f} \ll \frac{1}{T_{slowestpole}}$

The first condition states that the cut off frequency of the filter must be smaller than the the critical frequency of the closed loop system, given the controller C. This condition let us approximate by design the transfer function between y and v to the transfer function between y1 and v around the critical frequency ω_c. Therefore it is possible to tune C only taking into consideration G1.

$$\frac{y}{v} \approx \frac{y1}{v} \tag{4.5}$$

The second condition states that the cut off frequency of the filters must be smaller than the frequency associated to what in equation 4.4 was indicated as T_2. This is done so that those dynamics are always attenuated by the low pass filter and do not create instabilities.

The use of both sensor signals instead of only the internal temperature avoid the need of taking into account the difference in values that the heat capacity of the fluid assumes during the process. Also there are many uncertainties in the model of the RT that may have a significant weight. The first one is the convective heat exchange inside the wall of the RT between metal and fluid, and between fluid and fluid and PT100 sensor walls. Also it is important to note that by the end of the transient, the temperature set point reaches a value very close to the upper limit, about 370°C. Therefore controlling the walls with a high bandwidth, so that a perturbation does not cause the controller to increase too much their temperature, is of paramount importance.

4.3.2 RT control design

The control scheme of the RT is shown in figure 4.8.

We have four inputs for the controllers:

- TE2_0 represents the signal of the internal temperature sensor of the RT.

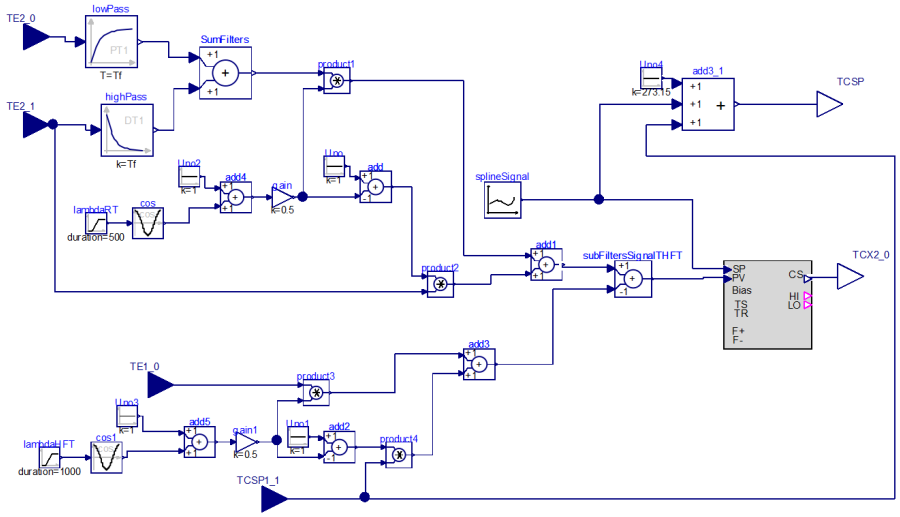

Figure 4.8: Overview scheme of the RT control design

- TE2_1 represents the signal of the thermocouple on the external wall of the RT.
- TE1_0 represents the signal of the internal temperature sensor of the HFT.
- TCSP1_1 represents the set point curve of the HFT.

The set point curve of the PI controller is shown in figure 4.9. The control scheme operates in three distinct phases. To these phases correspond different process variables that are fed to the controller. A linear convex combination transition, defined as follows, is used to switch between the three process variables.

$$PV = \lambda PV_2 + (1 - \lambda)PV_1 \tag{4.6}$$

Phase 1 goes from the beginning of the HFT heating until the opening of the HFT_Valve, tMV4. During this phase, inside all pipe sections, there is the highest degree of vacuum that is is possible to obtain. The set point curve represents the desired temperature differential of the external walls and the temperature set point of the HFT, i.e. the process variable is the following

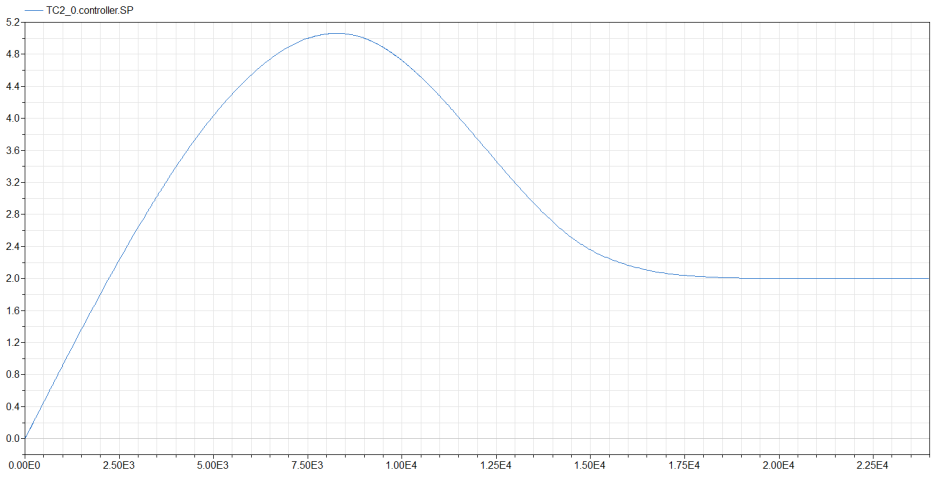

Figure 4.9: RT set point curve

$$PV_1 = TE2\_1 - TCSP1\_1 \tag{4.7}$$

The measurement of the internal temperature of the RT is not used since it would be unreliable at best since there is almost no fluid inside. The temperature differential reaches, at the end of phase 1, a maximum value TmaxSurr. This temperature differential is needed to guarantee that once the HFT_Valve is opened, at about 9000 s, the cooling of the fluid vapour that is expanding in all pipe sections does not cause the formation of condensate on the internal wall surface.

$$T_{internalwall}(t) > T_{fluidsaturation}(p(t)) \tag{4.8}$$

Phase 2 goes from the HFT_Valve opening to the end of the transient tmax, when the superheating value settles to Tsurr. The value of Tsurr shown in figure 4.9 is only used for the simulation. During the experimental campaign it would be changed accordingly.

The process variable is defined as follows:

$$PV_2 = (TE2\_1G_{HPF} + TE2\_0G_{LPF}) - TCSP1\_1 \tag{4.9}$$

Instead of using only the measurement of the fluid temperature, a combination of the low pass filtered fluid temperature measurement TC2_0 and the

high pass filtered external wall temperature TC2_1 is adopted as previously described.

Finally in phase 3 the process variable is defined as following:

$$PV_3 = (TE2\_1G_{HPF} + TE2\_0G_{LPF}) - TE1\_0 \tag{4.10}$$

Note that, instead of subtracting the HFT set point TCSP1_1 the temperature measurement T1.0 is used in order to obtain the highest possible accuracy for the superheating of the fluid.

This set point curve is obtained with a process similar to the one used to create the HFT set point curve: a matlab script is used to generate a set of points that a spline function in Dymola, or later the controller, uses to create the set point curve.

4.3.3 PI tuning

Since we are considering only the pipe walls in order to tune the controller, a better model of the pipe is used, obtained by linearizing a simplified model of the RT lacking external heat dissipation, internal fluid and thermal blankets. The state matrices are obtained linearizing the model. As expected the transfer function shows an integrator and numerous pole/zero pairs at similar frequencies.

A suitable PI is obtained using the Matlab Control System Toolbox.

4.4 CT temperature control

The control scheme of the heating jacket of a CT section is displayed In figure 4.10. Its purpose is to keep the external wall temperature of the CT section at the same temperature of the one of the reference tube.

We have two inputs for the controllers:

- TE2_1 represents the signal of the thermocouple on the external wall of the RT.

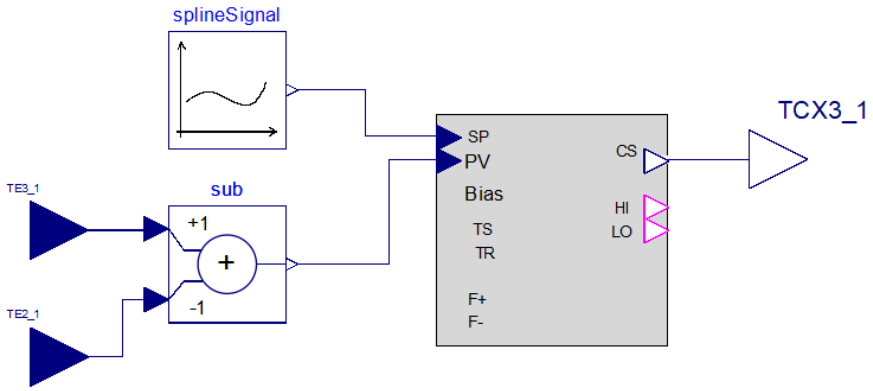

Figure 4.10: Overview scheme of the CT control design

- TE3_1 represents the signal of the thermocouple on the external wall of the CT.

This two inputs are used only for the purpose of the simulation since there is no measurement error to account for. The actual controller uses as process variable the voltage difference of the two thermocouples.

The process variable is as follows:

$$PV = TE3\_1 - TE2\_1 \tag{4.11}$$

The set point is, in this case, zero. As previously stated, the underlying assumption of the FAST apparatus is that the fluid inside the RT behaves like the one inside the CT so that imposing that the external walls of the CT are at the same temperature of the one of the RT means controlling the temperature of the fluid inside the charge tube.

Similarly to what was done for the reference tube, the state matrices of the simplified model of the CT are obtained linearizing the model so defined.

A suitable PI is obtained using the Control System Toolbox of Mathworks.

4.5 CTJ temperature control

In figure 4.11 is displayed the control scheme of the heating jacket of a charge tube joint CTJ. Its purpose is to keep the external wall temperature of the CT section at the same temperature of the one of the reference tube. Since the geometry of the joints is radically different from the one of the CT and RT some additional considerations are necessary.

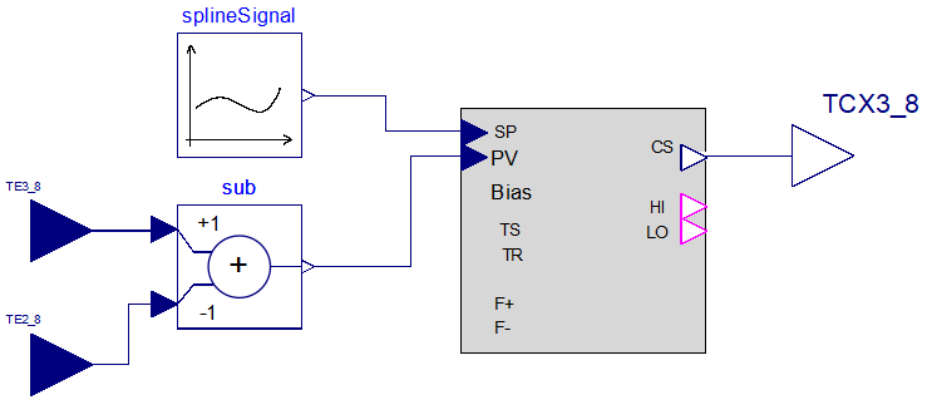

Figure 4.11: Overview scheme of the CTJ control design

We have two inputs for the controllers:

- TE2_8 represents the signal of the thermocouple on the external wall of the RT.
- TE3_8 represents the signal of the thermocouple on the external wall of the CTJ.

The process variable is as follows:

PV=TE3_8-TE2_8

The CTJ has a much bigger mass of metal, the tube section is 55mm thick while the CT and RT have a section of 15 mm. Consequently the assumption that is valid for the CT is not entirely valid for the joints.

The bigger mass of metal introduces a significant delay between the external wall temperature and the internal one.

Simulations show that this delay does not become significant during the heating of the experimental fluid except at the start of the simulation when the rate of heating of all the empty pipes is greater.

The proposal of the author of this thesis is to compensate this by simply adding an additional temperature delta, CTJoffset, to the set point of the external wall of the joints, see figure 4.12. The CTJoffset is then reduced until it reaches 0 by the end of the transient.

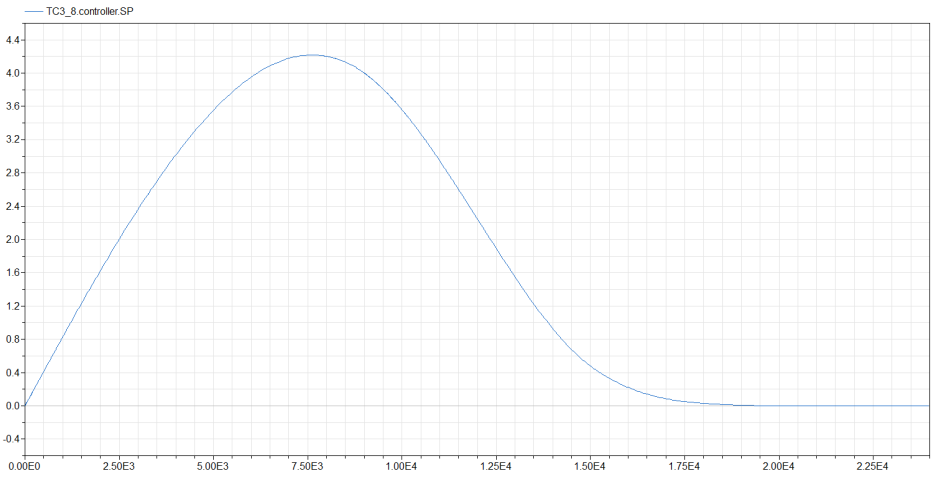

Figure 4.12: CTJ set point

Similarly to what was done for the reference tube and charge tube, the state matrices of the simplified model of the CT are obtained linearizing the model so defined.

A suitable PI is obtained using the Matlab Control System Toolbox.

4.6 Simulation results

The criteria used to evaluate the set points curve chosen and control design are the following:

1. Internal wall temperature always 3°C higher than Tsat during the transient so that condensation of fluid is not possible. At the end of

the transient this temperature delta will reach gradually the required superheating Tsurr.

2. No temperature overshoot higher than 1°C with respect to Tmax. As already discussed precedently, fluid degradation is to be avoided at all cost.

3. No saturation of the actuators. This is done to maintain controllability at all times. Additionally it is adopted as a criterion that all control signals must be lower than 80 % of nominal power available to keep some safety margin against modelling uncertainties.

4. Minimum time to desired fluid superheating (Tmax), tmax. A reasonable objective is that the FAST set up time be less than a 8-hour working day, so that at least one experiment per working day can be executed.

Below will be presented a series of simulation results showing that the criteria are fulfilled by all components of the FAST experimental apparatus. In the simulation the significant variables are the following:

- tMV4=9000 [s]
- tMax=21600 [s], 6 [h]
- Tmax=369 [°C]
- Tsurr=2 [°C]

The temperature difference between the internal wall temperature of the RT, CT and CTJ and the saturation temperature of the fluid is plotted in figure 4.13, 4.14 and 4.15. The condition is respected in all cases. It is important to note that before the HFTValve is opened the condition is not valid, but if there is condensation, it will be a negligible amount of condensate.

The fluid temperature in all three components and the overall set point TCSP is plotted In figure 4.16. The maximum overshoot is 0.5 [°C].

The behaviour of the control signals of the HFT controllers is plotted In figure 4.17, while the control signals of the controller of the RT, CT and CTJ are plotted in figure 4.18. The maximum output voltage for all control

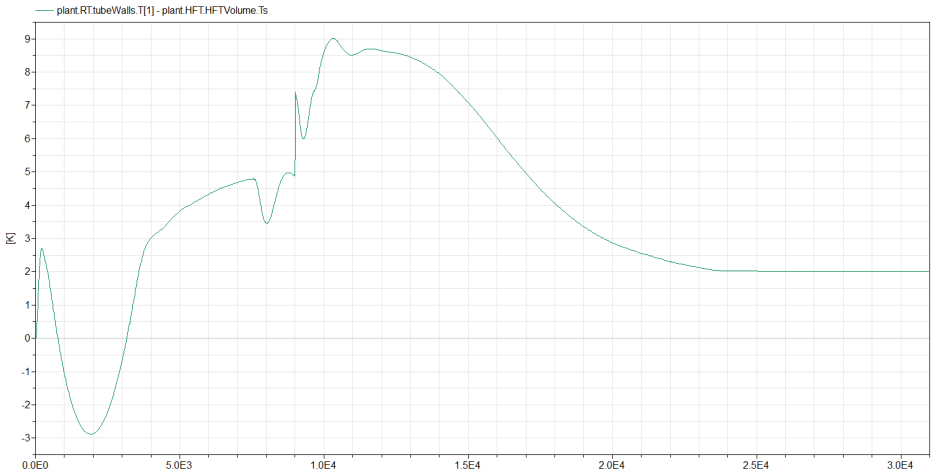

Figure 4.13: Temperature difference between RT internal walls and fluid saturation temperature

signals is 10 [V]. It is clearly visible that all heaters are underutilized except for the CTJ heating jacket that is pushed to the maximum allowed value, under the defined condition, before the HFT_Valve opening.

Finally, the total process takes about 6 hours and 40 minutes to reach an error of 0.025°C, see figure 4.19. A more precisely defined settling time can not be identified since the precision required by future experimental campaigns is not yet known. The settling time is well under the eight hours objective.

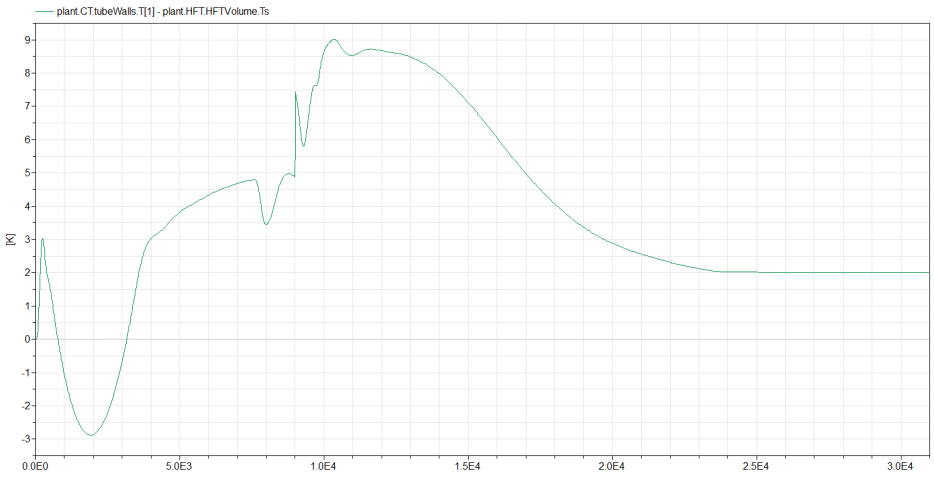

Figure 4.14: Temperature difference between CT internal walls and fluid saturation temperature

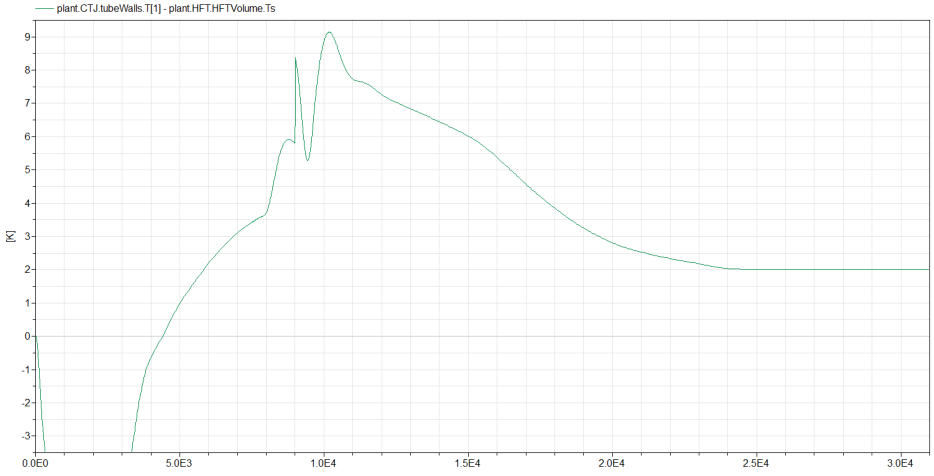

Figure 4.15: Temperature difference between CTJ internal walls and fluid saturation temperature

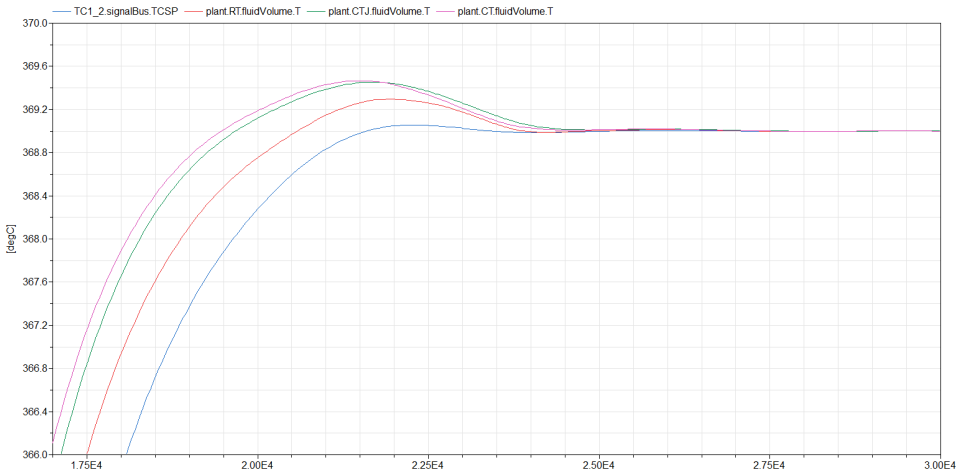

Figure 4.16: Fluid temperature behaviour at the end of the transient

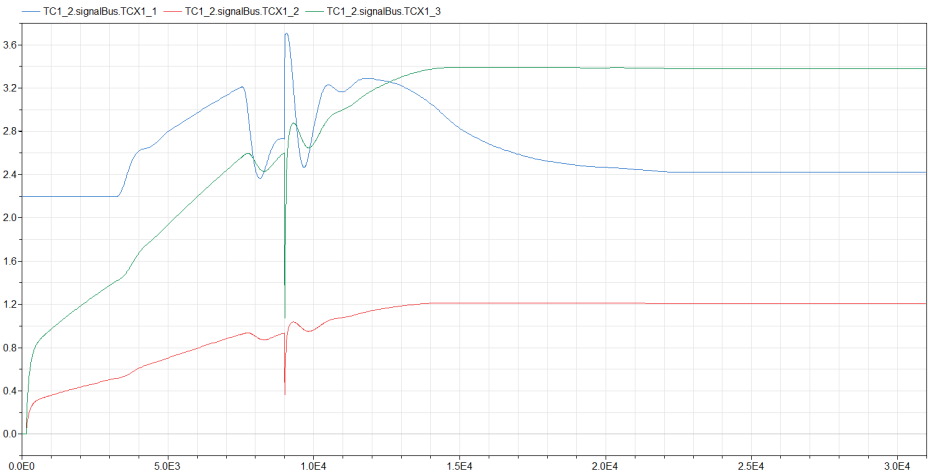

Figure 4.17: HFT control signals values

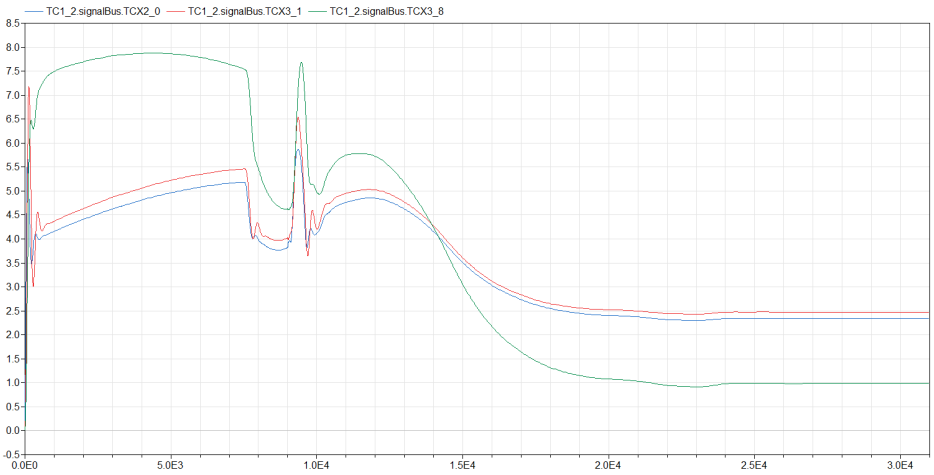

Figure 4.18: RT, CT and CTJ control signals values

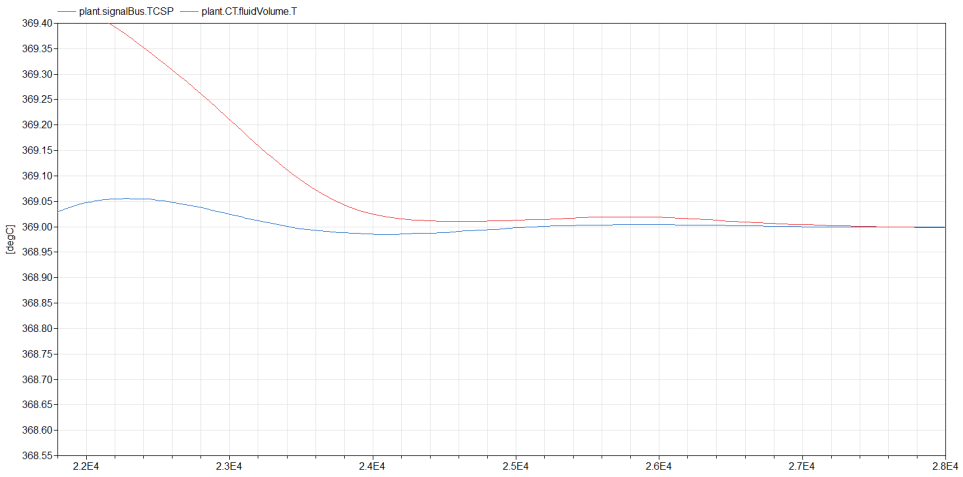

Figure 4.19: RT, CT and CTJ control signals values

Chapter 5

Conclusion and outlook

Two major changes to the control design of the FAST are proposed in this thesis:

1. A new control scheme for the temperature control of the reference tube.
2. A methodology for the definition of the set point curve of the vapour generator.

The proposed control scheme for the reference tube does not control precisely the temperature inside the RT until the end of the transient. This is obtained by combining the low pass filtered signal of the measured temperature inside the RC with the high pass filtered surface temperature of the RT walls. The advantages of this approach are numerous, chief among them the prevention of internal wall temperature overshoot if the fluid inside the RT lags behind the wall temperature. It is shown that by choosing a suitable filter cut off frequency T_f the dynamics due to the interaction with the fluid are strongly attenuated and the PI controller can be tuned up taking into account only the metal wall temperature transfer function. This proves advantageous since the model of the metal wall of the RT is well known and independent from the thermodynamic condition of the fluid while the fluid-wall interaction has numerous uncertainties.

The set point curve proposed for the HFT is a ramp with varying slope. At the end of the ramp a smooth juncture joins the ramp to the desired value

of T_{HFTmax}. This curve is generated by a Matlab script from a number of user defined parameters. By running simulations of the FAST model with different values for those parameters a good approximation of the best curve is obtained. This process highlights the bottlenecks of the system: the heaters on the charge tube joints are the only one maxed out until the opening of the HFT_Valve. Later on, no actuator is utilized at its maximum, therefore the bottleneck is the time needed for a smooth enough juncture that do not cause too much overshoot of the fluid temperature inside the tubes. Once the FAST model has been validated, this second bottleneck could be improved by using an optimization algorithm.

Before implementing any change proposed in this thesis it will be necessary to validate the model on the FAST facility, that at the time of writing of this thesis, is being assembled once again after having been moved to a new lab. First, the modelling hypothesis will need to be verified as sufficiently correct. Afterwards the parameters used on the model need to be calibrated by some open loop test. Finally the control architecture, controllers tuning and set point tuning will have to be tested.

Another improvement on the FAST facility that it is being evaluated is the introduction of forced recirculation of part of the fluid. By spilling some of the fluid at the end of the charge tube, condensing it and pumping it back to the HFT, the natural convection between fluid and metal wall that constitutes one of the uncertainties of the FAST would be substituted with forced convection that would lead to a much more predictable behaviour of the experimental apparatus. The model presented in this thesis could easily be adapted to include this improvement.

Finally, it would also be possible to use this model to optimize warm-start experiments, after the FOV is already opened once. It would not be necessary to heat up the charge tube that would be already at the desired temperature.

Bibliography

[1] Y. Zel'dovich, *On the possibility of rarefaction shock waves*, Zh. Eksp. Teor. Fiz. **4**, 363 (1946). Addison-Wesley, Reading, Massachusetts, 1993.

[2] P. A. Thompson, *A fundamental derivative in gasdynamics*, Phys. Fluids **14**, 1843 (1971).

[3] Tiemo Mathijssen. *Experimental observation of non-ideal compressible fluid dynamics*
`https://repository.tudelft.nl`

[4] P. Colonna, T. P. van der Stelt, and A. Guardone, *FluidProp (Version 3.0): A program for the estimation of thermophysical properties of fluids*, `http://www.fluidprop.com/` (2012), a program since 2004.

[5] T. Mathijssen, M. Gallo, E. Casati, N. Nannan, C. Zamfirescu, A. Guardone, and P. Colonna, *The flexible asymmetric shock tube (FAST), a Ludwieg tube facility for wave propagation measurements in high-temperature vapours of organic fluids*, J. Fluid Mech. (2015).

[6] F. Casella and A. Leva, *Modelica open library for power plant simulation: Design and experimental validation*, in Proceedings 3rd International Modelica Conference, edited by P. Fritzson (Modelica Association, Linköping, Sweden, 2003) pp. 41—50.

[7] F. Casella and A. Leva, *Modelling of thermo-hydraulic power generation processes using Modelica*, Math. Comput. Modell. Dyn. Syst. 12, 19 (2006).

[8] F. Casella and C. C. Richter, *ExternalMedia: a library for easy re-use of external fluid property code in Modelica, in Proceedings 6th International Modelica Conference*, edited by B. Bachmann (Modelica Association, Bielefeld, Germany, 2008) pp. 157—161.

[9] Nawin Ryan Nannan. *Advancements in non classical gas dynamics* `https://repository.tudelft.nl`

Appendix A

Matlab script

```
   (clear all
close all
clc
clearvars

maxTime=6*3600;
int=1800;
maxTimeRT=maxTime-int;
MV4opening=9000;
TValve=257;
interval=1000; %interval for TC 2.0 set point
rowNumber=26;
rowNumber2=16;
rowNumber3=8;
maxT=367; %steaty state maximum saturation temperature of HFT
steadySurr=2; %superheating at maxTime
steadySurrCTJ=0; %temperature offset of CTJ at steady state
CTJoffset=4; %temperature offset of CTJ at MV4opening
maxSurr=5; %maximum superheating imposed by the RT set point
table=zeros(rowNumber,2);
table2=zeros(rowNumber2,2);
table3=zeros(rowNumber3,2);
rate2=(maxSurr-steadySurr)/(maxTimeRT-MV4opening);
rateCTJ=(CTJoffset-steadySurrCTJ)/(maxTimeRT-MV4opening);
```

```
ratexstandard=0.01640364; %standard ramp rate to cross the MV4opening
ratex=ratexstandard*0.95;
intm=100;
intf=1800;
ratea=(257-25)/MV4opening;
rateb=(maxT-257)/(maxTime-MV4opening);
tflat1=1200;
tflat2=1000;

% %Independent equations that define the spline a and b coefficients:

% a*ratea*(MV4opening-tflat1-3*intm)+tflat1*ratex+(a*ratea+(ratex-...
% a*ratea)*1/4)+(a*ratea+(ratex-a*ratea)*2/4)+(a*ratea+(ratex-a*ratea)*...
% 3/4)=Tvalve-25
%
% b*rateb*(maxTime-5*intf-3*intm-MV4opening-tflat2)+ratex*tflat2+...
% (0.027+0.071+0.181+0.42+0.786)*b*rateb*intf+[ratex+(ratex-b*rateb)/...
% 4*1]*intm+[ratex+(ratex-b*rateb)/4*2]*intm+[ratex+(ratex-b*rateb)/4*3]*...
% intm=maxT-Tvalve;


%a and b are the modifiers to the standard slope rate ratea and rateb

a=(257-25-tflat1*ratex-3/2*ratex*intm)/(ratea*(MV4opening-tflat1-3*intm)...
    +3/2*ratea*intm);


b=(maxT-257-ratex*tflat2-3/2*ratex*intm)/(rateb*(maxTime-MV4opening-...
    5*intf-tflat2-3*intm)+3/2*rateb*intm+(1.485)*rateb*intf);




%% HFT Set Point

table(1,1)=0;
table(1,2)=25;

table(2,1)=MV4opening-3*intm-tflat1;
```

```
table(2,2)=a*ratea*(MV4opening-3*intm-tflat1)+25;

table(3,1)=MV4opening-2*intm-tflat1;
table(3,2)=(a*ratea+(ratex-a*ratea)/4*1)*intm+table(2,2);

table(4,1)=MV4opening-1*intm-tflat1;
table(4,2)=(a*ratea+(ratex-a*ratea)/4*2)*intm+table(3,2);

table(5,1)=MV4opening-tflat1;
table(5,2)=(a*ratea+(ratex-a*ratea)/4*3)*intm+table(4,2);

table(6,1)=MV4opening;
table(6,2)=ratex*tflat1+table(5,2);

table(7,1)=MV4opening+tflat2;
table(7,2)=ratex*tflat2+table(6,2);

table(8,1)=MV4opening+tflat2+intm;
table(8,2)=(ratex+(b*rateb-ratex)/4*1)*intm+table(7,2);

table(9,1)=MV4opening+tflat2+2*intm;
table(9,2)=(ratex+(b*rateb-ratex)/4*2)*intm+table(8,2);

table(10,1)=MV4opening+tflat2+3*intm;
table(10,2)=(ratex+(b*rateb-ratex)/4*3)*intm+table(9,2);

table(11,1)=maxTime-5*intf;
table(11,2)=b*rateb*(maxTime-5*intf-MV4opening-tflat2-3*intm)+table(10,2);

table(12,1)=maxTime-4*intf;
table(12,2)=b*rateb*0.786*intf+table(11,2);

table(13,1)=maxTime-3*intf;
table(13,2)=b*rateb*0.42*intf+table(12,2);

table(14,1)=maxTime-2*intf;
table(14,2)=b*rateb*0.181*intf+table(13,2);

table(15,1)=maxTime-1*intf;
table(15,2)=b*rateb*0.071*intf+table(14,2);
```

```
table(16,1)=maxTime;
table(16,2)=b*rateb*0.027*intf+table(15,2);


for i=17:rowNumber
    table(i,1)=maxTime+(i-16)*int;
    table(i,2)=maxT;


end


%% Set Point Surriscaldamento RT




table2(1,1)=0;
table2(1,2)=0;

table2(2,1)=MV4opening;
table2(2,2)=maxSurr;

table2(3,1)=maxTimeRT-5*interval;
table2(3,2)=steadySurr+rate2*(0.027+0.071+0.181+0.42+0.786)*interval;

table2(4,1)=maxTimeRT-4*interval;
table2(4,2)=steadySurr+rate2*(0.027+0.071+0.181+0.42)*interval;

table2(5,1)=maxTimeRT-3*interval;
table2(5,2)=steadySurr+rate2*(0.027+0.071+0.181)*interval;

table2(6,1)=maxTimeRT-2*interval;
table2(6,2)=steadySurr+rate2*(0.027+0.071)*interval;

table2(7,1)=maxTimeRT-1*interval;
table2(7,2)=steadySurr+rate2*(0.027)*interval;

for i=8:rowNumber2
```

```
    table2(i,1)=maxTimeRT+(i-8)*interval;
    table2(i,2)=steadySurr;
end

%% Set Point Surriscaldamento aggiuntivo CTJ

table3(1,1)=0;
table3(1,2)=0;

table3(2,1)=MV4opening;
table3(2,2)=CTJoffset;

table3(3,1)=maxTimeRT-5*interval;
table3(3,2)=steadySurrCTJ+rateCTJ*(0.027+0.071+0.181+0.42+0.786)*interval;

table3(4,1)=maxTimeRT-4*interval;
table3(4,2)=steadySurrCTJ+rateCTJ*(0.027+0.071+0.181+0.42)*interval;

table3(5,1)=maxTimeRT-3*interval;
table3(5,2)=steadySurrCTJ+rateCTJ*(0.027+0.071+0.181)*interval;

table3(6,1)=maxTimeRT-2*interval;
table3(6,2)=steadySurrCTJ+rateCTJ*(0.027+0.071)*interval;

table3(7,1)=maxTimeRT-1*interval;
table3(7,2)=steadySurrCTJ+rateCTJ*(0.027)*interval;

for i=8:rowNumber2
    table3(i,1)=maxTimeRT+(i-8)*interval;
    table3(i,2)=steadySurrCTJ;
end)
```